

# What Cell Size Does the Computed Slope/Aspect Angle Represent?

Michael E. Hodgson

## Abstract

The computation of slope and aspect angles for a cell is a common procedure in environmental studies and remote sensing applications in which topography is important. While the algorithm for computing slope/aspect angles requires either four or eight neighbors in a centered three by three window of cells, the estimated angles are used as if they depict the surface orientation of only the single central cell. Two questions result from this observation. What cell size does the slope and aspect angle derived from this window best represent? How different is the actual surface angle of the central cell from the surface angle computed using the window of elevation values? Although this difference in computation versus use is somewhat known, it has never been documented. This article empirically demonstrates that the slope/aspect angle derived from the neighboring elevation points best depicts the surface orientation for a larger cell—either 1.6 times or 2.0 times larger than the size of the central cell. It is suggested that, rather than first resampling elevation datasets of a finer resolution to a larger cell size commensurate with other data in a study and then deriving slope/aspect angles, a mean slope/aspect angular measurement be derived directly from the higher resolution data for each larger cell size.

## Introduction

Surface slope and aspect are commonly used by-products of an elevation surface for a wide variety of applications. Sometimes the elevation grid used is a resampling from a finer elevation grid to a coarser elevation grid so that the cell sizes of different data layers are commensurate. This resampling process may be throwing away information important in the slope/aspect computation. The computation of slope/aspect for each surface cell is made from some number of neighboring elevation values in a three by three window but is used as if it represents the surface angles for only the central cell. It is often assumed that the computed surface angles actually represent a cell size twice as large as the original grid cell. Although this difference in computation versus use is somewhat known, the representative cell size has never been documented. Further, the magnitudes of error which exist between the use of the angle for a one cell area and the actual angle for that cell are not well understood. In other words, are the angles all that different?

Using a well-known synthetic surface, this paper empirically determines the cell size that the bi-directional surface normal computed from elevation values in a three by three window actually represents. Three different slope/aspect algorithms are examined with three different grid-cell sizes.

The results indicate that the estimated surface normal from the four nearest neighboring cells in a three by three window best models the surface of a cell 1.6 times as large as the sampling interval in the elevation grid. For slope/aspect algorithms using the eight nearest neighbors in a three by three window, the actual cell represented is about 2.0 times the sample interval. These relationships are consistent regardless of the sample interval in the original elevation grid.

## Methodology

The size of the grid cell portrayed by the elevation surface sampling interval and the cell size that is best represented by the estimated angle from a 3 by 3 matrix of elevation values will be hereafter referred to as the *grid-cell size* and *representative cell size*, respectively. Determining the representative cell size will involve a continuous range of candidate representative cell sizes. The examination between grid-cell size and representative cell size was conducted using a mathematically defined synthetic terrain surface. A mathematically defined surface allows perfect definition of the elevation points on the surface and near-perfect<sup>1</sup> estimation of the mean surface normal of any size cell on the surface. To demonstrate the difference in angles estimated by slope/aspect algorithms using different numbers of neighbors, three commonly used algorithms were tested. Because estimation of surface properties is sensitive to the sampling intensity, three different grid-cell sizes were also examined.

## The Test Surface

This study used the 49-term trigonometric surface by Morrison (1971; 1974) as the synthetic terrain surface to compare each representation cell size and algorithm (Figure 1). The surface is a complex repeating series of undulations with a maximum slope of 60.48 degrees. Based on a preliminary examination of the surface, cell sizes of 50 by 50, 100 by 100, and 200 by 200 units were selected to represent different sampling intensities.

The true surface normal for the grid cell was computed using a pseudo-integrative approach—the vector mean surface normal of a finer sample of the elevation surface within each cell. This subsample is a 21 by 21 matrix of elevation

<sup>1</sup>The estimation of the true surface slope/aspect is "near-perfect" because it is approximated with a pseudo-integrative logic.

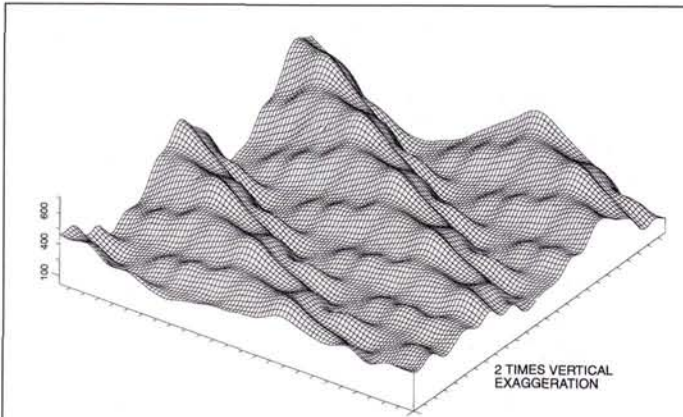


Figure 1. A perspective view of the synthetic surface used to compare actual and estimated surface orientation. The surface is generated by using a 49-term trigonometric series after Morrison (1971; 1974). The original surface from Morrison's work was rotated 50 degrees to avoid bias in the ridges running east-west. Tick marks are at a 200-unit spacing.

values (Figure 2a). Each subcell in the 21 by 21 subsample is 1/21th the size of the candidate representative cell size under investigation. (The 1/21th subsample is based on an empirical test that found a negligible difference in angular measurements using a smaller subcell size.) As an example, 441 subcells of 2.38 by 2.38 units in size were used to estimate the mean surface normal of a cell 50 by 50 units in size. When examining the 200- by 200-unit cell size, 441 subcells of 9.52 by 9.52 units in size were used to compute the vector mean.

To determine the cellsize represented by the bi-directional surface normal derived from the 3 by 3 grid-cell submatrix, a comparison was undertaken between this angle and the angles from a continuous range of candidate representative cell sizes from 0.1 to 3.0 times the size (along one axis) of the grid cell. Each candidate representative cell was centered at the same location as the grid cell, and the pseudo-integrative approach for computing the true surface angles was performed. A random sample of 50 grid cells on the elevation surface (Figure 1) was used in determining the mean angular error for each candidate representative cell size. The representative cell size was taken as that candidate cell size exhibiting the least mean angular error.

#### Bi-Directional Surface Normal

To avoid the problems associated with undefined aspect of "flat" slopes, bi-directional surface angles were used in this analysis rather than independent angles of slope and aspect. Bi-directional angles are also better indicators of surface orientation for applications such as the estimation of solar insolation or the topographic normalization of remotely sensed images. Slope/aspect is computed from the normal vector of a plane surface based on the cross products of two vectors in orthogonal axes on the surface. The slope in two orthogonal gradients, typically west-to-east (*we*) and south-to-north (*sn*), are used for this estimation: i.e.,

$$\text{Slope}^\circ = \text{Tan}^{-1} (\sqrt{\text{Slope}_{we}^2 + \text{Slope}_{sn}^2}) \quad (1)$$

The aspect of the surface was computed from an algorithm using the change in elevation values in the *we* and *sn* gradients (see algorithm in Ritter (1987)).

The bi-directional surface normal of a cell may be represented as a vector of unit length in *x-y-z* hemispherical space: i.e.,

$$\vec{N}_{\text{cell}} = [x, y, z] \quad (2)$$

$$\begin{aligned} \text{where } x &= \sin \text{ aspect} * \sin \text{ slope} \\ y &= \cos \text{ aspect} * \sin \text{ slope} \\ z &= \cos \text{ slope} \end{aligned}$$

For those instances when the slope of an observation is 0.0 (and, thus, the aspect angle is "undefined"), the coordinate locations for the vector endpoint are set to  $x = 0.0$ ,  $y = 0.0$ , and  $z = 1.0$ . This allows "flat" surfaces to be included in the computation of the vector mean.

#### Vector Mean Surface Normal

An algebraic average of bi-directional surface normal measurements from a number of surface angle observations is not possible because aspect angles are measurements on a circular scale, not a linear scale. However, after work in other fields on directional statistics (Rayleigh, 1880; Watson, 1966; Agterberg, 1974; Gaile and Burt, 1980), the vector mean was used as a "mean" surface orientation. The vector mean representing the surface normal in this 21 by 21 matrix of subcells was computed by adding the vector endpoints for each observation: i.e.,

$$\vec{N}_{\text{representative}} = \sum_1^{441} \vec{N}_i \quad (3)$$

#### Error in Surface Normal Angle

The bi-directional angular difference ( $bi_z$ ), or angular error, between the surface normals for a candidate cell size and the grid-cell size was derived from

$$bi_z = \cos^{-1} \left[ \frac{\vec{N}_{\text{representative}} \cdot \vec{N}_{\text{cell}}}{|\vec{N}_{\text{representative}}| * |\vec{N}_{\text{cell}}|} \right] \quad (4)$$

#### Slope/Aspect Algorithms

The fundamental differences between most slope/aspect algorithms is in the *number* of neighboring cell values used and the *weighting* of each cell value. The most common algorithms use either four or eight of the neighbors in a three by three window centered on the cell in question (Figure 2b). When using all eight neighbors, variations in algorithms use different weights for the diagonal neighbors. This study used one algorithm employing four nearest neighbors, a finite-difference algorithm using eight nearest neighbors, and a regression plane fitted to the eight nearest neighbors.

A commonly used algorithm that estimates surface angles from only the four nearest neighboring elevation values in the grid was suggested by Fleming and Hoffer (1979) and presented in algorithmic form by Ritter (1987): i.e.,

$$\text{Slope}_{sn} = \frac{e_4 - e_2}{2 * \text{cell size}}; \quad \text{Slope}_{we} = \frac{e_1 - e_3}{2 * \text{cell size}} \quad (5)$$

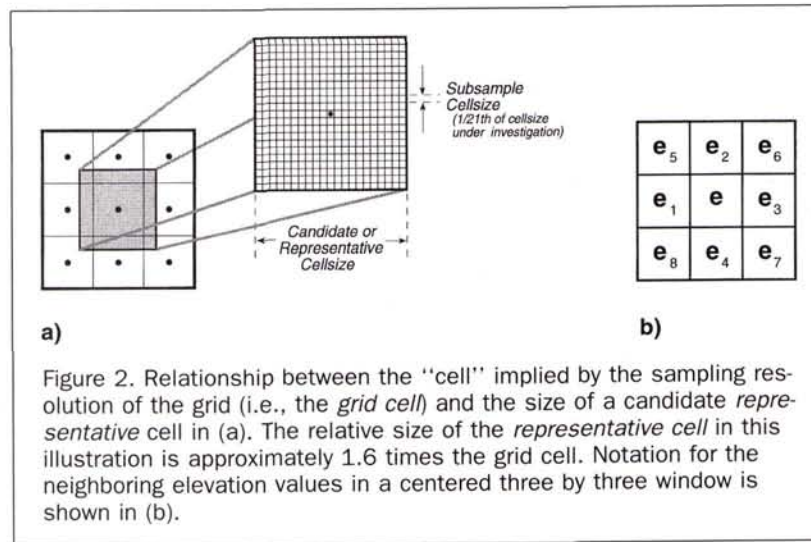


Figure 2. Relationship between the "cell" implied by the sampling resolution of the grid (i.e., the *grid cell*) and the size of a candidate *representative cell* in (a). The relative size of the *representative cell* in this illustration is approximately 1.6 times the grid cell. Notation for the neighboring elevation values in a centered three by three window is shown in (b).

where  $e_i$  = elevation value of the 3 by 3 submatrix (Figure 2b).

A third-order finite difference method using eight neighboring elevation values (by differencing the set of elevations on opposite sides of the central cell) was suggested by Sharpnack and Akin (1969): i.e.,

$$\begin{aligned} \text{Slope}_{sn} &= \frac{(e_7 + e_4 + e_8) - (e_6 + e_2 + e_5)}{6 * \text{cell size}}; \\ \text{Slope}_{wr} &= \frac{(e_8 + e_1 + e_5) - (e_7 + e_3 + e_6)}{6 * \text{cell size}}. \end{aligned} \quad (6)$$

The method suggested by Sharpnack and Akin produces the same results as a multiple linear regression model (or a least-squares fitted plane to the eight elevation values), yet is computationally more efficient.

Horn (1981) presented a modified version of Sharpnack and Akin's method using unequal weights for the closer elevation values: i.e.,

$$\begin{aligned} \text{Slope}_{sn} &= \frac{(e_7 + 2e_4 + e_8) - (e_6 + 2e_2 + e_5)}{8 * \text{cell size}}; \\ \text{Slope}_{wr} &= \frac{(e_8 + 2e_1 + e_5) - (e_7 + 2e_3 + e_6)}{8 * \text{cell size}}. \end{aligned} \quad (7)$$

### Results and Implications

The results of the tests indicate a direct and stable relationship between the grid-cell size and the representative cell size. The representative cell size was found to be either 1.6 or 2.0 times the grid-cell size, depending on the number of neighbors used in the slope/aspect algorithm (Figure 3). The surface normal produced from the algorithm that used only four neighboring values was most closely associated with a representative cell about 1.6 times the grid-cell size (Figure 4). The other two algorithms<sup>2</sup> using eight neighbors were most closely associated with a representative cell size approximately 2.0 times the grid-cell size. This relationship be-

<sup>2</sup>The regression algorithm produced angles that represented a cell size slightly larger—close to 2.1 times the grid-cell size.

tween algorithm and representative cell sizes was consistent regardless of the grid-cell size (or relative surface sampling intensity). It would be expected that this relationship would hold true for any study area and sampling intensity.

What may be surprising is (1) the magnitude of error between the representative cell size and grid-cell size surface angles and (2) the relative accuracy between algorithms. The average bi-directional angular error between estimated and true surface angles at the 1.0 cell size (i.e., the cell size such measures are used to represent) ranged from 0.74 to 1.51, 2.30 to 4.68, and 7.45 to 9.50 degrees for the 50-, 100-, and 200-unit cell sizes, respectively (Figure 3 and Table 1). The low mean angular error for the smaller cell sizes was expected and indicates the similarity of surface angles in close proximity to each observation. If the surface angles derived from the 3 by 3 window were actually used for the representative cell size (1.6 or 2.0 times larger cell sizes) the average error would only range from 0.48 to 0.65, 1.37 to 1.93, and 1.91 to 4.08 degrees. Thus, it is suggested that the error in surface normal angles may be reduced by a factor of from two to four by computing surface angles with finer resolution data but using these computed angles to represent coarser resolution data. Obviously, the magnitude of error could be lesser or greater for other data sets and cell sizes.

The algorithm using four neighboring values was consistently more accurate for estimating surface angles at the grid-cell size (i.e., the 1.0 candidate cell size). For instance, the mean angular error at the 50- by 50-units grid-cell size was only 0.74 degrees for the four neighbor algorithm but was 1.26 and 1.51 degrees for the two eight neighboring algorithms. This finding was true for each of the three grid-cell sizes examined. Thus, in the typical application where the surface normal angles are used to represent the grid-cell size, the algorithm using only four neighbors should be used. This finding is in contrast to the work by Skidmore (1989), who determined that the eight-neighbor algorithms were more accurate than the four-neighbor algorithm. The methodology used by Skidmore for defining truth, however, included an estimation of "true" slope/aspect angles from a contour map where all eight neighboring values were used to manually estimate surface angles.

One implication of this study would suggest that eleva-

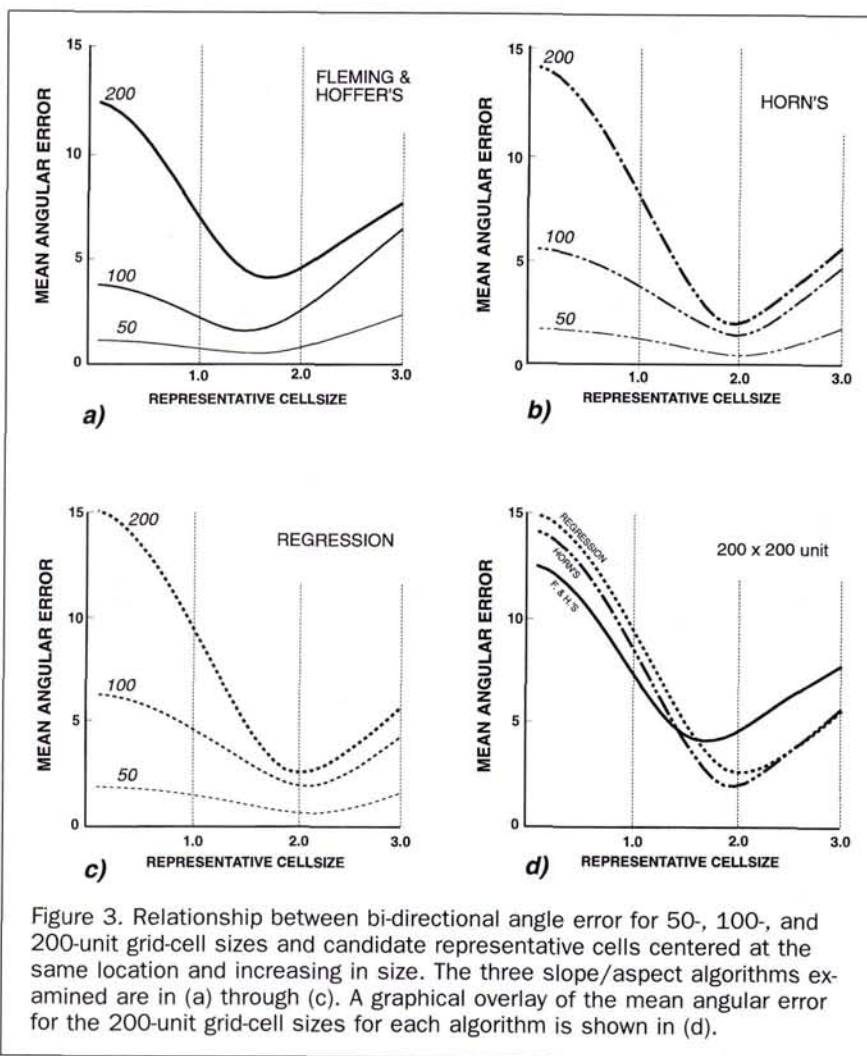


Figure 3. Relationship between bi-directional angle error for 50-, 100-, and 200-unit grid-cell sizes and candidate representative cells centered at the same location and increasing in size. The three slope/aspect algorithms examined are in (a) through (c). A graphical overlay of the mean angular error for the 200-unit grid-cell sizes for each algorithm is shown in (d).

tion data be collected at a higher spatial sampling intensity than the other data layers in an application. In other applications, where the elevation data must be generalized to a coarser sample size, it may be desirable (and likely more accurate) to determine the slope/aspect angles for the larger cells from a vector mean of the smaller cell sizes. Slope/aspect angles could be derived for the grid-cell size of this greater sampling intensity, and then the slope/aspect surface(s) could be resampled to the coarser resolution of the other data layers using some vector mean interpolation method. For instance, rather than using 30- by 30-m elevation data to derive slope/aspect angles for a study that also uses 30- by 30-m Thematic Mapper imagery, one might use an elevation layer sampled at 5 m by 5 m or 15 m by 15 m. Slope/aspect angles representing 30- by 30-m cell sizes may be computed utilizing a vector mean from an elevation grid of 5- by 5-m cell sizes during the resampling process. However, other empirical tests are required to determine appropriate methods for weighting each observation and for developing an interpolation function. The selection of the ideal cell size, however, is problematic because one often relies on available elevation data, such as U.S. Geological Survey or Defense Mapping Agency derived data. The availabil-

ity of softcopy photogrammetry and stereo photography may allow the analyst greater freedom to determine the sampling

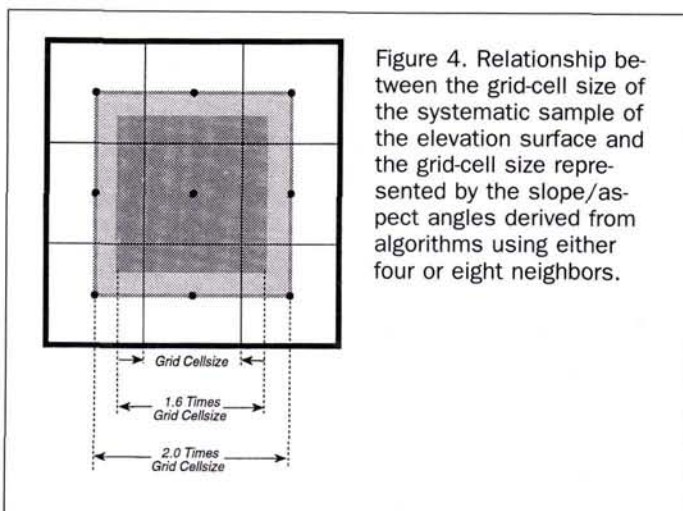


Figure 4. Relationship between the grid-cell size of the systematic sample of the elevation surface and the grid-cell size represented by the slope/aspect angles derived from algorithms using either four or eight neighbors.

TABLE 1. MEAN HEMISPHERICAL ANGULAR ERROR AT DIFFERENT CANDIDATE CELL SIZES FOR ALGORITHM AND GRID-CELL SIZE COMBINATIONS (ERROR IN DEGREES)

Candidate Cellsize <sup>1</sup>	Flemming/ Hoffer's			Horn's			Regression		
	50	100	200	50	100	200	50	100	200
0.1	1.07	3.76	12.42	1.64	5.51	14.09	1.88	6.22	14.86
0.2	1.06	3.71	12.23	1.62	5.45	13.89	1.87	6.17	14.66
0.3	1.04	3.62	11.91	1.60	5.37	13.56	1.85	6.08	14.34
0.4	1.02	3.51	11.49	1.58	5.25	13.11	1.82	5.97	13.90
0.5	0.98	3.36	10.96	1.54	5.10	12.56	1.79	5.82	13.35
0.6	0.94	3.19	10.36	1.50	4.92	11.92	1.74	5.64	12.71
0.7	0.90	2.99	9.69	1.45	4.71	11.20	1.70	5.43	11.99
0.8	0.85	2.78	8.97	1.39	4.47	10.41	1.64	5.20	11.21
0.9	0.80	2.54	8.22	1.33	4.22	9.57	1.58	4.95	10.37
1.0	0.74	2.30	7.45	1.26	3.94	8.69	1.51	4.68	9.50
1.1	0.68	2.06	6.70	1.19	3.65	7.79	1.44	4.39	8.60
1.2	0.63	1.84	6.00	1.10	3.34	6.87	1.36	4.08	7.68
1.3	0.58	1.66	5.37	1.02	3.03	5.96	1.27	3.77	6.78
1.4	0.53	1.54	4.85	0.93	2.71	5.07	1.18	3.46	5.89
1.5	0.50	<b>1.51</b>	4.44	0.83	2.41	4.22	1.09	3.15	5.06
1.6	<b>0.48</b>	1.54	4.18	0.73	2.11	3.45	0.99	2.85	4.30
1.7	0.49	1.66	<b>4.08</b>	0.64	1.85	2.77	0.90	2.58	3.63
1.8	0.54	1.84	4.11	0.56	1.63	2.23	0.82	2.33	3.09
1.9	0.62	2.09	4.25	0.50	1.45	1.95	0.75	2.13	2.72
2.0	0.72	2.40	4.47	<b>0.45</b>	<b>1.37</b>	<b>1.91</b>	0.69	1.98	<b>2.57</b>
2.1	0.84	2.74	4.77	<b>0.45</b>	1.44	2.05	<b>0.65</b>	<b>1.93</b>	2.58
2.2	0.98	3.13	5.09	0.51	1.61	2.34	0.66	1.97	2.71
2.3	1.12	3.53	5.43	0.59	1.87	2.69	0.70	2.10	2.93
2.4	1.27	3.95	5.77	0.71	2.21	3.08	0.77	2.30	3.21
2.5	1.43	4.37	6.11	0.85	2.60	3.49	0.86	2.53	3.55
2.6	1.59	4.79	6.43	1.00	3.00	3.90	0.96	2.80	3.91
2.7	1.76	5.22	6.75	1.17	3.41	4.32	1.09	3.12	4.30
2.8	1.94	5.64	7.07	1.34	3.82	4.74	1.24	3.47	4.71
2.9	2.12	6.05	7.38	1.52	4.23	5.16	1.40	3.84	5.12
3.0	2.30	6.46	7.69	1.70	4.64	5.58	1.57	4.21	5.55

<sup>1</sup>The candidate cell size is given as a fraction of the regular tessellation in the elevation model. For instance, a candidate cell size of 1.6 at the 50- by 50-m grid-cell size is 80 by 80 m.

resolution (under the limitation of the quality of and base/height ratio of the photography).

References

Agterberg, F.P., 1974. Calculation of Preferred Orientations from Vectorial Data, *Geomathematics: Mathematical Background and Geo-Science Applications*, Elsevier Scientific Publishing Company, New York, pp. 475-508.

Fleming, M.D., and R.M. Hoffer, 1979. *Machine Processing of Landsat MSS Data and DMA Topographic Data for Forest Cover Type Mapping*, LARS Technical Report 062879, Laboratory for Appli-

cations of Remote Sensing, Purdue University, West Lafayette, Indiana.

Gaile, G.L., and J.E. Burt, 1980. *Directional Statistics*, University of East Anglia, Norwich.

Horn, B.K.P., 1980. Hill Shading and the Reflectance Map, *Proceedings of the IEEE*, 69(1):14-47.

Morrison, J.L., 1971. *Method-Produced Error in Isarithmic Mapping*, Technical Monograph No. CA-5, American Congress on Surveying and Mapping, Washington, D.C.

———, 1974. Observed Statistical Trends in Various Interpolation Algorithms Useful for First Stage Interpolation, *The Canadian Cartographer*, 11(2):142-159.

Rayleigh, L., 1880. On the Resultant of a Large Number of Vibrations of the Same Pitch or Arbitrary Pause, *Philosophical Magazine*, 10:73-78.

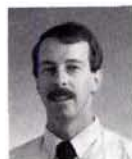
Ritter, P., 1987. A Vector-Based Slope and Aspect Generation Algorithm, *Photogrammetric Engineering & Remote Sensing*, 53(8):1109-1111.

Sharpnack, D.A., and G. Akin, 1969. An Algorithm for Computing Slope and Aspect from Elevations, *Photogrammetric Engineering*, 35(3):247-248.

Skidmore, A.K., 1989. A Comparison of Techniques for Calculating Gradient and Aspect from a Gridded Digital Elevation Model, *International Journal of Geographical Information Systems*, 3(4): 323-334.

Watson, G.S., 1966. The Statistics of Orientation Data, *Journal of Geology*, 74:787-797.

(Received 7 June 1993; accepted 14 September 1993; revised 8 October 1993)



Michael E. Hodgson

Michael E. Hodgson is a member of the research staff and is a Team Leader for the Geographic Research and Applications team in the GIS & Computer Modeling Group at the Oak Ridge National Laboratories (ORNL). He holds a B.A. degree from the University of Tennessee and both the M.S. and Ph.D. in Geography from the University of South Carolina. Prior to his position at ORNL, Dr. Hodgson was a faculty member at the University of Colorado from 1987 to 1994, where he researched computational analysis problems and human responses to natural hazards. Also at Colorado, he was the Principal Investigator on an NSF award that converted the Geography Department's PC based GIS/remote sensing teaching lab to a 15-workstation teaching/research laboratory. His specific research interests include the use of remote sensing and GIS methods for mapping and monitoring environmental changes. Current research activities include the characterization of environmental hazards, regional modeling of ecosystem processes, and knowledge-based information extraction.

Would you like to see your company's imagery on the cover of PE&RS?

Cost is \$2,000.

Call Joann Treadwell, ASPRS Director of Publications  
301-493-0290; fax 301-493-0208; email jtread@asprs.org